LncRNA *lnc-RI* regulates homologous recombination repair of DNA double-strand breaks by stabilizing *RAD51* mRNA as a competitive endogenous RNA

Liping Shen[1,2], Qi Wang[2], Ruixue Liu[2], Zhongmin Chen[2], Xueqing Zhang[2], Pingkun Zhou[1,2,*] and Zhidong Wang[2,*]

[1]School of Radiation Medicine and Protection, Medical College of Soochow University, Collaborative Innovation Center of Radiation Medicine of Jiangsu Higher Education Institutions, Suzhou, Jiangsu 215123, PR China and [2]Department of Radiation Toxicology and Oncology, Beijing Key Laboratory for Radiobiology, Beijing Institute of Radiation Medicine, Beijing 100850, PR China

ABSTRACT

DNA double-strand break (DSB) repair is critical for the maintenance of genome stability. The current models of the mechanism of DSB repair are based on studies of DNA repair proteins. Long non-coding RNAs (lncRNAs) have recently emerged as new regulatory molecules, with diverse functions in biological processes. In the present study, we found that expression of the ionizing radiation-inducible lncRNA, *lnc-RI*, was correlate negatively with micronucleus frequencies in human peripheral blood lymphocytes. Knockdown of *lnc-RI* significantly increased spontaneous DSBs levels, which was confirmed to be associated with the decreased efficiency of homologous recombination (HR) repair of DSBs. The expression of RAD51, a key recombinase in the HR pathway, decreased sharply in *lnc-RI*-depressed cells. In a further investigation, we demonstrated that miR-193a-3p could bind with both *lnc-RI* and *RAD51* mRNA and depressed the expression of *lnc-RI* and *RAD51* mRNA. *Lnc-RI* acted as a competitive endogenous RNA (ceRNA) to stabilize *RAD51* mRNA via competitive binding with miR-193a-3p and release of its inhibition of *RAD51* expression. To our knowledge, this is the first study to demonstrate the role of *lnc-RI* in regulating HR repair of DSBs. The feedback loop established in the current study suggests that *lnc-RI* is critical for the maintenance of genomic stability.

INTRODUCTION

Genome instability, which is defined as an increased frequency of mutations within the genome of a cellular lineage compared with the normal state, is a double-edged sword: on one hand, genome instability contributes to genetic diversity and biological evolution, while on the other hand, it plays a critical role in the pathology of many genetic-related diseases, including carcinogenesis (1–4). Human genome instability is also a major factor in some neurodegenerative diseases (5,6) and aging (7). Genome instability can be caused by multiple biological processes, including replication dysfunction, failure of DNA repair, and site-specific hotspots of genomic instability, as well as normal cell physiology and metabolism (8). Many genes encoding a series of proteins involved in maintaining genome stability, including those involved in DNA replication, post-replicative repair, DNA damage repair, DNA damage checkpoints, apoptosis, telomere maintenance or mRNA biogenesis, have been well described, and mutations or expression dysregulation of these genes have been confirmed to be associated with carcinogenesis (8–11).

Aberrations in the repair of DNA damage is an important cause of genomic instability (8). DNA double-strand breaks (DSBs) are considered to be the most catastrophic changes in the integrity of the genome during the life-span of a cell and are generally caused by conditions such as replication stress, genotoxic chemicals, ionizing radiation exposure, inflammation, oxidative stress and viral infection (4,12,13).To deal with these continuously produced lesions, eukaryotic cells have developed a complex and efficient DNA damage response (DDR) system, including numerous DNA damage repair pathways, disruption of which has disastrous effects on the genome (4,8,10).Homologous recombination (HR) and non-homologous end-joining(NHEJ) are the major molecular pathways responsible for DSB repair. The NHEJ pathway is an error-prone mechanism, initiated by the binding with the DNA-PK complex to the DNA break ends. In contrast, HR is an error-free repair

pathway that involves the use of homologous DNA sequences as templates in the late S and G2 phases. This process is highly conserved across species ranging from yeast to humans, and occurs via a series of precisely controlled events. In HR repair, the RAD51 protein (phage UvsX, bacterial RecA or archaeal RadA) is the central recombinase responsible for homologous pairing and the DNA strand exchange reaction in an ATP-dependent manner (14,15).The fidelity of RAD51 expression is critical in avoiding illegitimate recombination events during HR that may lead to genetic instability. This recombinase is known to mediate positive and negative regulation at the post-translational level by multiple molecules including BRCA1, BRCA2, PLK1, RAD51 paralogs, or other regulators (16–19). For example, phosphorylation of RAD51 by PLK1 at serine 14(S14) can activate its function in HR repair via enhanced interaction with the MRE11–RAD50–NBS1 (MRN) complex (18).

Long non-coding RNAs (lncRNAs) are a group of non-coding RNA transcripts comprising more than 200 nucleotides and lacking apparent open reading frames. LncRNAs play important roles in many cellular biological processes, including cell cycle progression, apoptosis, development, pluripotency of stem cells, muscle differentiation and carcinogenesis (20–25). According to the competing endogenous RNA (ceRNA) hypothesis, specific RNAs can act as sinks for pools of miRNAs to control the expression of other transcripts targeted by these miRNAs, and lncRNAs are essential components of the ceRNA cross-talk process (26). Some lncRNAs are now emerging as regulators of DDR. LncRNA *LIRR1*, *gadd7* and *lincRNA-p21* were reported to regulate DDR by activating the G1/S checkpoint (27–29). Several lncRNAs have also been revealed to affect DSB repair. Zhang et al. reported that the lncRNA *LINP1* contributed to NHEJ by serving as a molecular scaffold between Ku80 and DNA-PKcs (30). *PCAT-1*, a characterized prostate cancer lncRNA, was demonstrated to have a significant inhibitory effect on HR activity by interacting directly with the 3′UTR of the *BRCA2* gene and mediating consequent post-transcriptional repression of *BRCA2* (31). LncRNA *DDSR1* is a DNA damage-inducible lncRNA that positively regulates HR repair by interacting with BRCA1 and hnRNPUL1. Defects in *DDSR1* have been shown to lead to aberrant DSB repair (32). *TODRA*, another HR pathway-regulating lncRNA, was reported to promote HR efficiency in a *RAD51*-dependent manner by regulating both RAD51 expression and activity (33). *Lnc-RI* (long noncoding RNA radiation induced; Gene ID: 401296) with1423 nucleotides encoded by a gene located in chromosome 7p22.3 (ENST00000382528) is first identified in our laboratory as a radiation-inducible lncRNA. Our previous study indicated that *lnc-RI* is involved in the control of mitosis by regulating *PLK1* expression via competitive targeting of miR-210-3p (34). In that study, an interesting phenomenon was revealed in that knockdown of *lnc-RI* led to aberrant expression of a set of DDR regulators, indicating that *lnc-RI* may play a role in DDR and genomic instability.

In the present study, we have revealed the role of *lnc-RI* in regulating the HR pathway of DSB repair and maintaining genomic stability. It was found that *lnc-RI* expression correlated negatively with micronucleus frequencies in the peripheral blood lymphocytes of healthy adults. *Lnc-RI* knockdown led to significantly increased levels of spontaneous DSBs in human cell lines and depression of HR efficiency. Furthermore, HR recombinase RAD51 expression was suppressed by silencing of the *lnc-RI* gene. Finally, our results indicated that miR-193a-3p targets both *RAD51* and *lnc-RI*, and that *lnc-RI* regulates the stability of *RAD51* mRNA by competitively binding with miR-193a-3p and relieving its inhibition of *RAD51* mRNA. Our findings reveal a novel mechanism of HR pathway regulation by *lnc-RI* via the *lnc-RI*/miR-193a-3p/*RAD51* mRNA 3′UTR axis.

MATERIALS AND METHODS

Isolation of peripheral blood lymphocytes for RNA extraction

Human peripheral blood samples were collected from 21 healthy donors (13 males and 8 females; aged 24–68 years). Written informed consent was obtained from all participant and the protocol was approved by the Ethics Subcommittee on Human Investigation of the Beijing Institute of Radiation Medicine (China). Peripheral blood lymphocytes were isolated from 4 ml EDTA-anticoagulated peripheral blood collected from each person by centrifugation at a speed of 1000 rpm for 20 min using lymphocyte separation medium (Hao Yang Biotechnology company, Tianjin, China). Cell pellet was washed by 10 mL 0.9% sodium chloride solution through repeated centrifugation at the same speed for 15 min and total RNA was extracted using TRIzol reagent (Sigma, USA) according to the manufacturer's instructions.

CB micronucleus assay

Heparin-anticoagulated whole blood samples (1 ml) were collected from each participant and CB micronucleus assays were performed according to a previously described method (35). One thousand randomly selected binucleate cells per donor were counted to quantify the micronucleus frequency among peripheral blood lymphocytes using an Olympus BX61 microscope (model: BX61TRF; Japan). Micronucleus frequencies were calculated according to the following formula:

$$\text{Micronucleus frequency } (\text{‰})$$
$$= \frac{n(\text{number of micronucleus})}{N(\text{number of binucleate cells})} \times 1000; N = 1000.$$

Cell culture

All cell lines used in this study were maintained in our laboratory and cultured at $37°C$ in a humidified incubator under 5% CO_2: HeLa cells were cultured in RPMI-1640 medium (HyClone, USA); MCF-7 and LO2 cells were cultured in high glucose DMEM medium (HyClone, USA); U2OS cells were cultured in McCoy's 5A medium (HyClone, USA); U2OS cells containing the GFP HR assay construct were cultured in high glucose DMEM medium (HyClone, USA). All media were supplemented with 10% prime fetal bovine serum (ExCell Bio, Cat. No. FSP500, China), penicillin (100 units/ml) and streptomycin (100 μg/ml).

Primers, probes, siRNAs and miRNA mimics

Primers, probes, siRNA duplexes and miRNA mimics used in this study were synthesized by Shanghai GenePharma Company (Shanghai, China). Details of the sequences are shown in Supplementary Tables S1–S3.

Transfection

Cells were transfected with 100 nM siRNA or miRNA mimics using Lipofectamine 2000 (Invitrogen, USA). For transfection with plasmids, cells were plated in six-well plates (3.0 × 10^5 cells/well) ∼24 h before transfection with 2.5 μg plasmids per well.

Lentivirus preparation and infection

Lentiviruses expressing shRNA-*lnc-RI* (LV-KD-*lnc-RI*) or negative control oligonucleotide sequences shRNA-NC (LV-NC) were prepared by GenePharma (Shanghai, China). The details of shRNA sequences are shown in Supplementary Table S4. HeLa cells were infected with lentivirus at a multiplicity of infection (MOI) of 20 in the presence of polybrene at a final concentration of 5 μg/ml. After 72 h, the cells were cultured in selection medium containing puromycin (1.5 μg/ml) for 7 days. The stably infected cells were then cultured continuously in RPMI-1640 medium supplemented with 0.5 μg/ml puromycin.

Actinomycin D (CHD) or cycloheximide (CHX) exposure

HeLa cells stably infected with 20 MOI lentivirus (LV-KD-*lnc-RI* or LV-NC) were exposed to 5 μg/ml CHD for 0, 1, 2, 4, 6 or 8 h to block transcription; absolute ethanol was used as the control reagent. Quantitative real-time PCR was performed to analyze *RAD51* mRNA expression levels. HeLa cells were exposed to 100 μg/ml CHX for 0, 1, 2, 4, 8 or 12 h to block translation; dimethyl sulfoxide (DMSO) was used as the control reagent. RAD51 protein expression levels were evaluated by western blot analysis.

RNA extraction and real-time PCR

Total RNA from cells were extracted by TRIzol Reagent (Sigma, USA) according to the manufacturer's instructions. Quality control of the isolated RNA was determined with an ultraviolet spectrophotometer (GE Healthcare GeneQuant 100, USA). 1 μg RNA was employed to synthesize cDNAs using PrimeScriptRT reagent kit with gDNA Eraser (TaKaRa, Japan). TaqMan probe-based real-time PCR analyses were performed on the Bio-Rad MyiQ™2 platform using SuperReal PreMix (Probe) (TIANGEN, China). PCR reactions were performed in a 25 μl volume in triplicate. Amplification steps as follows: step1, initial denaturation at 95°C for 15 min; step 2, denaturation at 95°C for 3 s; step 3, anneal at 60°C for 30 s; 40 cycles form step 2 to step 3. β-Actin was used as a normalizer in the real-time PCR and the relative expression of evaluated genes were calculated by $2^{-\Delta\Delta CT}$ method.

Western blot analysis

Cells were harvested by 0.25% trypsin digestion and washed twice with ice cold phosphate-buffered saline (PBS). Cell pellets were lysed in lysis buffer (50 mM Tris–HCl, pH 7.5; 150 mM NaCl; 0.5% sodium deoxycholate; 1% NP-40) containing protease inhibitors and phosphatase inhibitors at the concentrations recommended by the manufacturer for 30 min in ice bath. SDS-PAGE and western blotting were performed to analyze the cell lysates according to standard protocols. The following antibodies were used in western blot analyses: phospho-histone H2AX (Ser139) monoclonal antibody (Millipore, USA; Cat. No. 05-636, 1:1000); β-Actin monoclonal antibody (Proteintech, USA; Cat. No. 60008-1-lg, 1:2000); PLK1 monoclonal antibody (Santa Cruz Biotechnology, USA; Cat. No. sc-17783, 1:500); RAD51 polyclonal antibody (Proteintech; Cat. No. 14961-1-AP, 1:2000); BRCA2 polyclonal antibody (Proteintech; Cat. No. 19791-1-AP, 1:500); NBS1 polyclonal antibody (Proteintech; Cat. No. 55025-1-AP, 1:2000); RAD50 polyclonal antibody (Ruiyingbio, China; Cat. No. RLT3963, 1:500); MRE11 polyclonal antibody (Ruiyingbio; Cat. No. RLT2829, 1:1000); BRCA1 polyclonal antibody (Ruiyingbio; Cat. No. RLT0519, 1:500); BCL2 monoclonal antibody (Ruiyingbio; Cat. No. RLT0519, 1:1000).

Immunofluorescence

Cells were cultured on coverslips in six-well plates (2.5 × 10^5 cells/well). At 24 h or 48 h post-transfection, HeLa and U2OS cells were fixed in 4% formaldehyde for 15 min at room temperature, permeabilized in 0.3% Triton X-100-PBS buffer and then blocked in 3% bovine serum albumin for 1 h at room temperature. Cells were stained using standard procedures. Specifically, cells were incubated with phospho-histone H2AX (Ser139) monoclonal antibody (Millipore, USA; Cat. No. 05-636, 1:500) at 4°C overnight in a humidifier, and then washed twice in PBS. Subsequently, cells were incubated with a FITC-labeled anti-IgG antibody (KPL, USA; Cat. No. 02-15-06, 1:250) at room temperature for 2 h. DNA was stained with DAPI at a concentration of 2 μg/ml for 10 min in the dark. Images were obtained using a Nikon Ti-A1 capture system (magnification, 60×).

Comet assay

The neutral comet assays were performed using the Reagent Kit for Single Cell Gel Electrophoresis Assay (Trevigen, USA, Cat. No. 4250-050-K) according to the manufacturer's instructions. DNA was stained using 100 μl propidum iodide (PI, 2 μg/ml) per slide at room temperature for 30 min in the dark. Images were obtained using the Olympus BX61 capture system (magnification, 20×). In each group, 50–100 cells were quantified using CaspLab software.

DR-GFP/I-Sec I HR assay

HR assays of U2OS-DR-GFP were performed as previously described (36). U2OS-DR-GFP cells (provided by Dr T. Ma) were first transfected with 100 nM siRNA-*lnc-RI*

or siRNA-NC followed by I-Sec I expressing plasmids (or control vectors) in 8 h later using Lipofectamine 2000 according to the manufacturer's instructions. After 72 h, cells were harvested and the percentage of GFP-positive (GFP+) cells was quantified by flow cytometry (BD FACSCalibur).

NHEJ assay

The mechanism of NHEJ activity assay was well described in Seluanov A and his colleagues' study (37). HeLa cells stably infected with lentivirus (LV-KD-*lnc-RI* or LV-NC) were co-transfected with pDsRed2-N1 plasmid which expressing red fluorescent protein (RFP) as transfection control, and NHEJ reporter plasmid which expressing green fluorescent protein (GFP) digested with Hind III, at a ratio of pDsRed2-N1: predigested NHEJ reptoter = 1:3, 2.5 μg total DNA per 3.0×10^5 cells. 48 h after transfection, the percentage of GFP+ and RFP+ cells were measured via flow cytometry (BD FACSCalibur). NHEJ activity in HeLa cells were evaluated by the percentage of GFP+ cells in RFP+ cells.

Dual luciferase reporter assay

RAD51 mRNA 3′UTR and *lnc-RI* sequences were cloned into the pGL3M vector to generate the pGL3M-*RAD51* 3′UTR and pGL3M-*lnc-RI* constructs. Subsequently, mutant sequences at the predicted target sites for miR-193a-3p in the *RAD51* mRNA 3′UTR or *lnc-RI* were cloned into the pGL3M vector to generate the pGL3M-*RAD51* 3′UTR-M and pGL3M-*lnc-RI*-M constructs. Cells were seeded into 24-well plates (6.0×10^4/well) for approximately 24 h before co-transfection with 10 ng of reporter plasmid and 1 ng pRL-CMV internal control plasmid. After 8 h, the medium was replaced and cells were transfected with 100 nM miRNA mimics. After incubation for 48 h, the transfected cells were lysed and luciferase activity was detected using a Dual-Luciferase Reporter Assay System (Promega, USA, Cat. No. E1910). Firefly luciferase activity was normalized to Renilla luciferase activity and each group was assayed in triplicate.

Statistical analysis

Spearman's correlation coefficient was calculated to assess the significance of the correlation between expression levels of lnc-RI and micronucleus frequency using Statistical Analysis System (SAS) ($P < 0.05$ was considered to indicate statistical significance). Data from real-time PCR, comet assay and flow cytometry data were presented as means±SD (all experiments were performed in triplicate or more). Experiments with two experimental groups were statistically analyzed using Two-tailed Student's *t*-tests. *$P < 0.05$, **$P < 0.01$ or ***$P < 0.001$ was considered to indicate statistical significance, n.s. meant no significance.

RESULTS

Negative correlation of *lnc-RI* expression with micronucleus formation

The micronucleus is formed in nucleated cells by chromosome breakage or loss and is generally recognized as a biomarker of genomic instability (38). Our previous findings indicated that *lnc-RI* is a radiation-inducible lncRNA molecule involved in radiation-induced DDRs. Therefore, we hypothesized that *lnc-RI* is associated with genome integrity. To test this hypothesis, we first investigated the potential relationship between *lnc-RI* expression and micronucleus frequency in peripheral blood lymphocytes of 21 healthy donors. The results of real-time PCR analysis of *lnc-RI* expression levels and analysis of micronucleus frequency using the cytokinesis-block (CB) micronucleus assay are presented in Table 1. The data of Figure 1 indicated that the micronucleus frequency correlated negatively with *lnc-RI* expression, which implicating that *lnc-RI* may involve in the maintenance of genome stability.

Knockdown of *lnc-RI* expression increased accumulation of spontaneous DSBs in multiple cell lines

Our previous study indicated that expression of some DDR-related genes was disrupted in *lnc-RI* knockdown cells (34). In present study, we found that promoter of *lnc-RI* contain NF-κB(p65) binding sites (between +71 bp and +81 bp) and then we confirmed that *lnc-RI* may be induced by radiation in a NF-κB(p65) dependent manner (see in Supplementary Figure S1). Next, we found that *lnc-RI* knockdown may sensitized HeLa cells to radiation (Supplementary Figure S2). Combined with data of Figure 1, we hypothesized that *lnc-RI* participates in the maintenance of genomic stability by regulating the efficiency of intrinsic cellular DNA repair processes. To test our hypothesis, *lnc-RI* expression in HeLa and U2OS cells was silenced using siRNA targeting technology. At 24 h or 48 h after transfection, cells were harvested for analysis of γ-H2AX expression and γ-H2AX foci, which are recognized markers of DSBs. Compared with siRNA-NC, siRNA-*lnc-RI* #1 and #2 effectively depressed expression of *lnc-RI* (Figure 2A), with significantly increased γ-H2AX and γ-H2AX foci formation (Figure 2B and C). Similar results were observed in MCF-7 and LO2 cells (Supplementary Figure S3). These results indicated that knockdown of *lnc-RI* expression significantly increases accumulation of spontaneous DSBs.

In further investigations, neutral comet assays were performed to detect the yield of DSBs in HeLa and U2OS cells at 24 h or 48 h after transfection with specific siRNAs. As shown in Figure 2D, DNA fragments were dramatically increased in the cells transfected with *lnc-RI*-specific siRNAs. We confirmed that knockdown of *lnc-RI* increased spontaneous DSBs levels in multiple cell types (Figure 2A–D, Supplementary Figure S3).

lnc-RI regulates homologous repair of DSBs by regulating *RAD51* expression

We investigated the effect of *lnc-RI* on HR activity of DSBs using a well-characterized HR reporter assay (DR-GFP) in U2OS cells. Compared with the control cells, *lnc-RI* knockdown resulted in a significant decrease in the GFP signal that represents the efficiency of HR repair of DSBs generated in the reporter construct by I-Sce I; *RAD51* knockdown cells was performed as a positive control (Figure 3A–C). At the same time, We also investigated the effect of *lnc-*
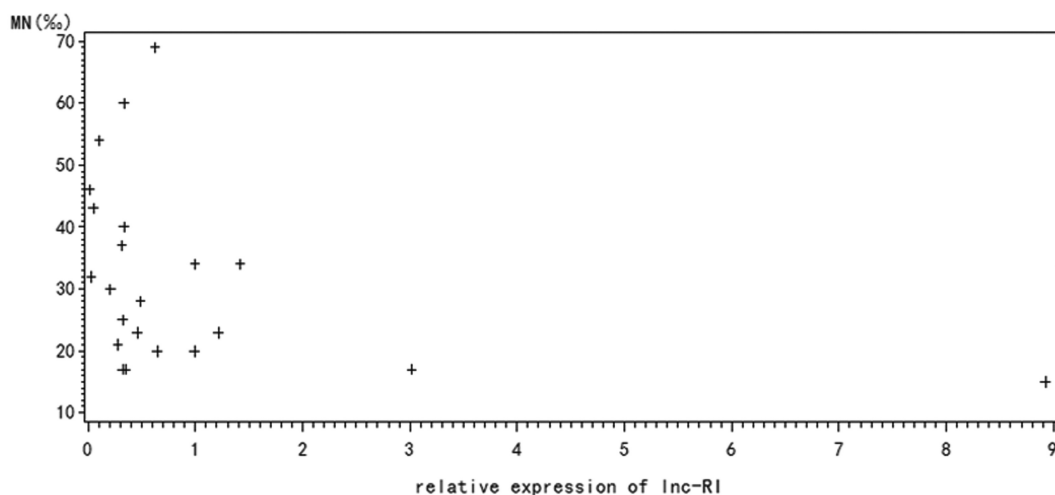
Figure 1. The correlation of *lnc-RI* expression and micronucleus frequency in human lymphocytes. CB micronucleus assays were used to measure the micronucleus frequency in human peripheral blood lymphocytes. 1000 randomly selected binucleated cells per sample were scored to calculate micronucleus frequency ($n = 21$). The correlation between *lnc-RI* expression and micronucleus frequency was tested by Spearman's correlation coefficient using SAS (Spearman correlation coefficient: –0.4409, $P < 0.05$).

Table 1. The expression of lnc-RI and micronucleus frequency in human peripheral blood lymphocytes

Individual	Gender	Age (years)	Relative expression of Lnc-RI	Micronucleus frequency(‰)
1	Female	25	8.93	15
2	Male	27	3.02	17
3	Male	25	0.36	17
4	Male	27	1.00	20
5	Female	25	0.65	20
6	Male	24	0.28	21
7	Male	26	1.21	23
8	Female	30	0.46	23
9	Male	24	0.32	25
10	Female	28	0.49	28
11	Male	26	0.21	30
12	Male	54	0.03	32
13	Male	62	1.42	34
14	Male	54	1.00	34
15	Male	68	0.32	37
16	Male	64	0.33	40
17	Female	61	0.05	43
18	Female	53	0.02	46
19	Female	63	0.11	54
20	Female	68	0.33	60
21	Female	55	0.63	69

RI on NHEJ activity of DSBs. Our result found that knockdown of lnc-RI may slightly inhibit NHEJ activity (Supplementary Figure S4).

Next, we try to identify the target of *lnc-RI* by which *lnc-RI* regulate HR activity, expression of several essential proteins in the HR pathway (MRE11, RAD50, NBS1, RAD51, BRCA1, BRCA2, PLK1 and BCL2) were detected by western blotting. As shown in Figure 3D–E, knockdown of *lnc-RI* in both HeLa and U2OS cells significantly depressed RAD51 and PLK1 expression. The expression of some HR pathway-associated proteins (RAD50, BRCA1, BRCA2) were also found to be depressed to some extent. Next, we over-expressed RAD51 and PLK1 in *lnc-RI* knockdown cells, only over expression of RAD51 could attenuate the level of γ-H2AX induced by *lnc-RI* knockdown (Supplementary Figure S5).

In Figure 3C, we found a interesting phenomenon: knockdown of *RAD51* also depressed expression of *lnc-RI*, which is confirmed in Supplementary Figure S6. Next, HCT116 cells (more sensitive to radiation than HT29 cells) and HT29 cells were selected. And the expression of *RAD51* and *lnc-RI* in HCT116 and HT29 were detected. As shown in Supplementary Figure S7, both levels of *lnc-RI* and *RAD51* in HT29 cells are higher than which in HCT116.

All these evidence above suggested that *RAD51* is a critical target through which *lnc-RI* plays a role in the HR pathway and give us a cue that lnc-RI may regulate *RAD51* expression as an ceRNA which is confirm in Figure 4, Figure 5 and Supplementary Figure S6.

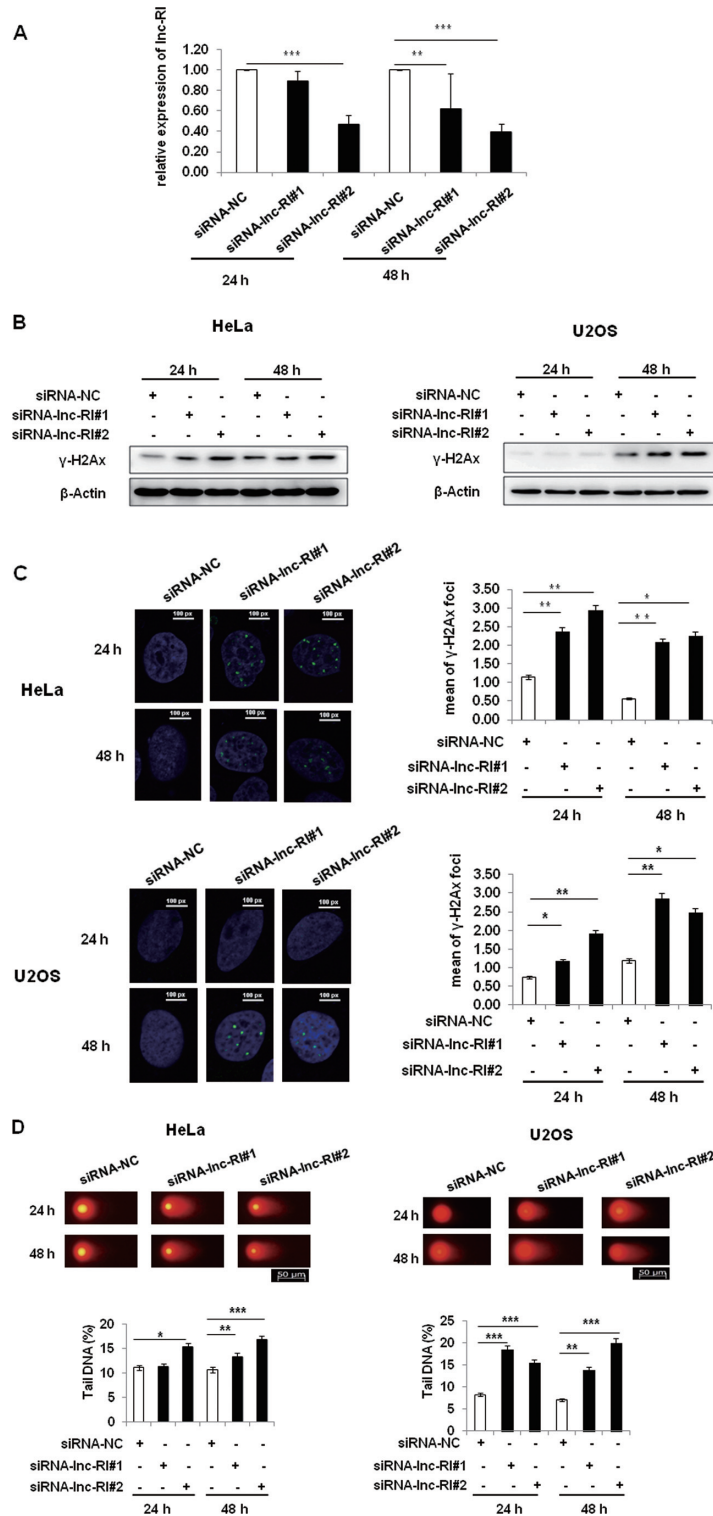**Figure 2.** Knockdown of *lnc-RI* led to increased levels of spontaneous DSBs in multiple types of cells. (**A**) SiRNA-mediated depression of *lnc-RI* expression. HeLa cells were transfected with 100 nM siRNA-*lnc-RI* or the control siRNA-NC. After 24 h and 48 h, *lnc-RI* expression was measured by real-time PCR. *t*-test, mean ± SD, $n = 3$. (**B**) *Lnc-RI* knockdown increased the expression of γ-H2AX. HeLa and U2OS cells were transfected with siRNA-*lnc-RI* or siRNA-NC. Expression of γ-H2AX was detected by Western blot analysis ($n = 6$). (**C**) *Lnc-RI* knockdown elicited γ-H2AX foci formation. HeLa and U2OS cells were transfected with siRNA-*lnc-RI* or siRNA-NC. γ-H2AX foci were detected by indirect immunofluorescence staining using an anti-γ-H2AX primary detection antibody and a FITC-conjugated anti-IgG secondary detection antibody; 200 randomly selected cells in each group were scored (*t*-test, mean ± SD, $n = 200$). (**D**) Comet assay analysis of DSBs induced by *lnc-RI* knockdown. HeLa and U2OS cells were transfected with equivalent concentrations of siRNA-*lnc-RI* or siRNA-NC. DNA fragments were detected by neutral comet assay performed 24 h and 48 h after transfection. Percentage of tail DNA in each group were measured by CaspLab software. *t*-test, mean±SD, $n = 50$–100. Scale bar, 50 μm. The comet assay were repeated three times. *$P < 0.05$, **$P < 0.01$, ***$P < 0.001$.
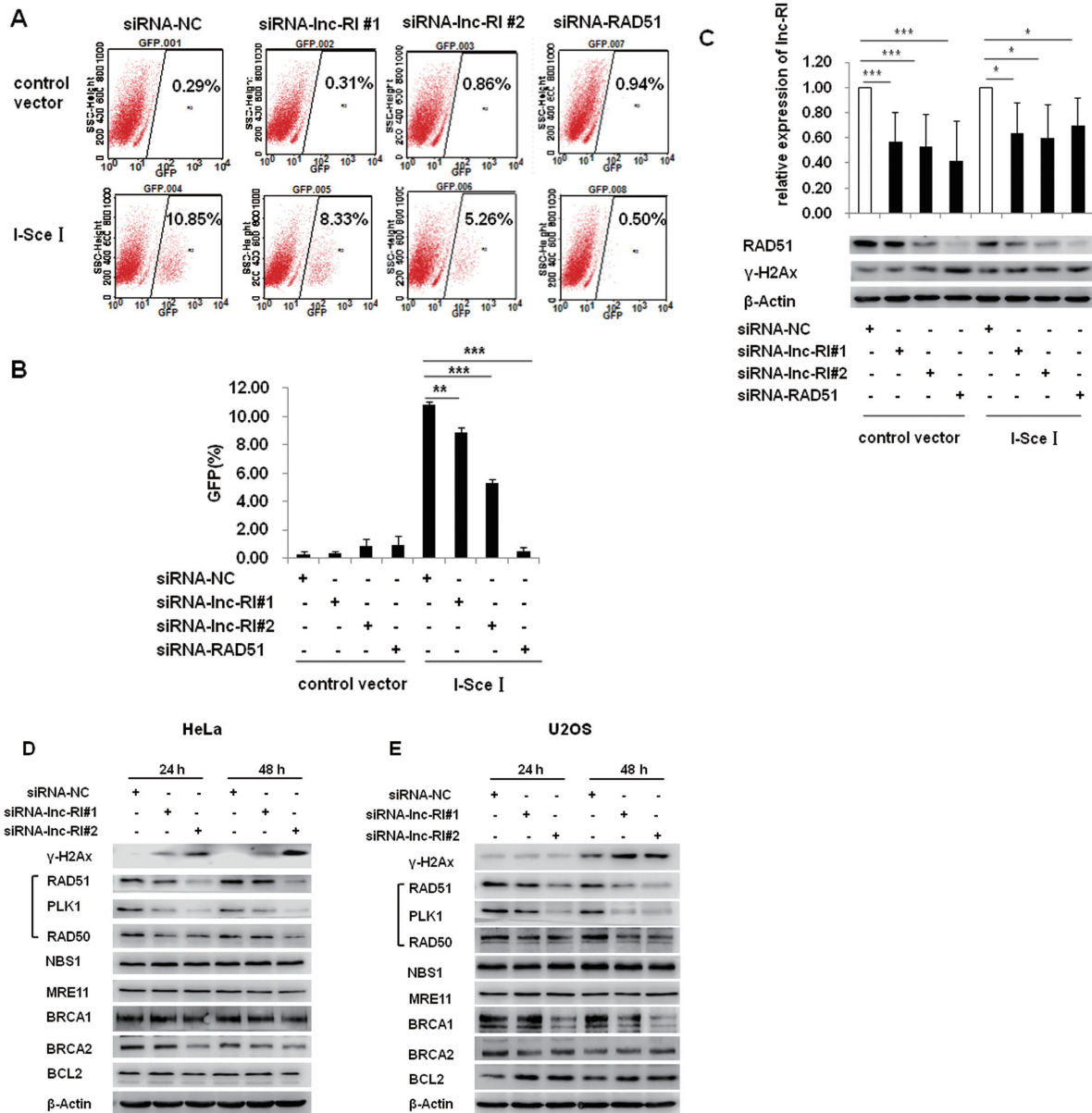
Figure 3. Knockdown of *lnc-RI* depressed HR efficiency. (A–C) knockdown of *lnc-RI* suppressed HR efficiency. DR-GFP U2OS cells were co-transfected with I-Sce I expressing plasmids and siRNA-*lnc-RI* or siRNA-NC. After 72 h, I-Sce I induced homologous recombination was detected via flow cytometry (**A**) and the results statistically analyzed. *t*-test, data are presented as mean ± SD, *n* = 3 (**B**). The expression of *lnc-RI* was analyzed by real-time PCR (*t*-test mean ± SD, *n* = 3) (**C**, top); the expression of RAD51 and γ-H2AX was analyzed by Western blot (**C**, bottom). (**D**, **E**) *Lnc-RI* knockdown decreased the expression of some essential components in HR pathway. HeLa (**D**) and U2OS (**E**) cells were transfected with siRNA-*lnc-RI* and siRNA-NC. After 24 and 48 h, cells were harvested and expression of HR-essential proteins was analyzed by Western blot. Western blot analysis were performed more than three times.*$P < 0.05$, **$P < 0.01$, ***$P < 0.001$.

Lnc-RI is necessary for the stabilization of *RAD51* mRNA

The mechanism by which *RAD51* depression is induced by *lnc-RI* knockdown was further investigated. RNAi-mediated *lnc-RI* knockdown in HeLa and U2OS cells resulted in decreased *RAD51* expression at both the protein and mRNA levels (Figure 4A; Supplementary Figure S8). Next, we investigated the ability of *lnc-RI* to regulate the stability of *RAD51* mRNA and protein. HeLa cells were infected with LV-KD-*lnc-RI* (or control lentivirus LV-NC). Western blot analysis at 1, 2, 4, 8 and 12 h after the addi-tion of cycloheximide (CHX) to block translation indicated that *lnc-RI* knockdown had no effect on the degradation of RAD51 protein (Figure 4B). In contrast, quantitative real-time PCR analysis after the addition of actinomycin D (CHD) to block transcription revealed rapid degradation of *RAD51* mRNA in *lnc-RI* knockdown cells (Figure 4C). These data indicated that *lnc-RI* is necessary for stabiliza-tion of *RAD51* mRNA.
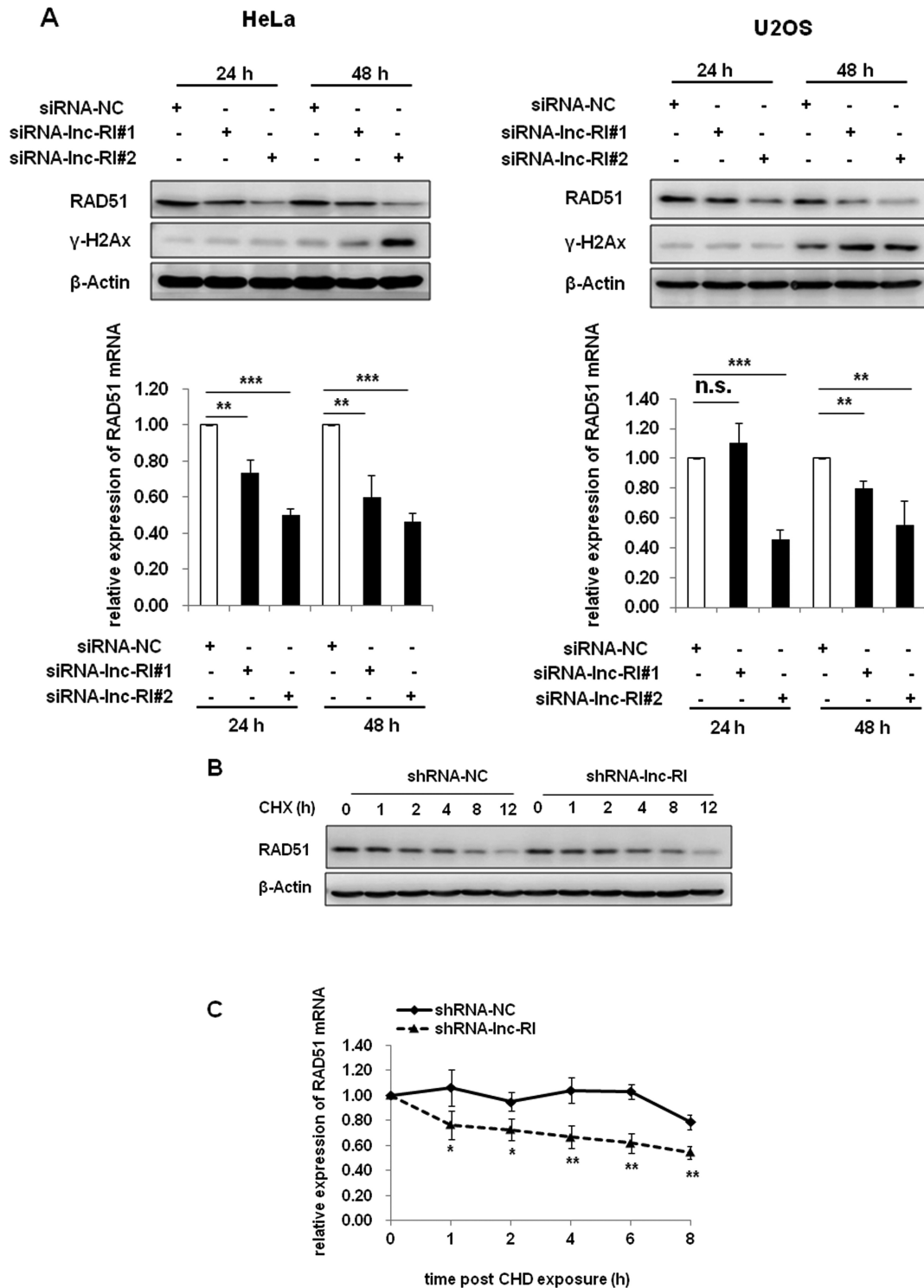
Figure 4. Knockdown of *lnc-RI* promoted the degradation of *RAD51* mRNA and decreased RAD51 protein levels. (**A**) *Lnc-RI* knockdown reduced *RAD51* gene expression at both the mRNA and protein levels. HeLa and U2OS cells were transfected with 100 nM siRNA-*lnc-RI* or siRNA-NC. After 24and 48 h, RAD51 protein and mRNA expression was detected by western blot (top) or real-time PCR (bottom), respectively. (**B**) *Lnc-RI* knockdown had no influence on degradation of RAD51 protein. RAD51 protein expression in HeLa cells infected with lentivirus LV-KD-*lnc-RI* (or LV-NC) was detected by Western blot at 0, 1, 2, 4, 8 and 12 h after the addition of 100 μg/ml CHX to bock translation. (**C**) *Lnc-RI* knockdown accelerated degradation of *RAD51* mRNA. *RAD51* mRNA expression in HeLa cells infected with the same lentivirus infected cells was detected by real time-PCR at 0, 1, 2, 4, 8, and 12 h after the addition of 5 μg/ml CHD to block transcription. These experiments were conducted on three independent occasions. *t*-test, mean ± SD, *$P < 0.05$, **$P < 0.01$, ***$P < 0.001$, n.s. means no significance.
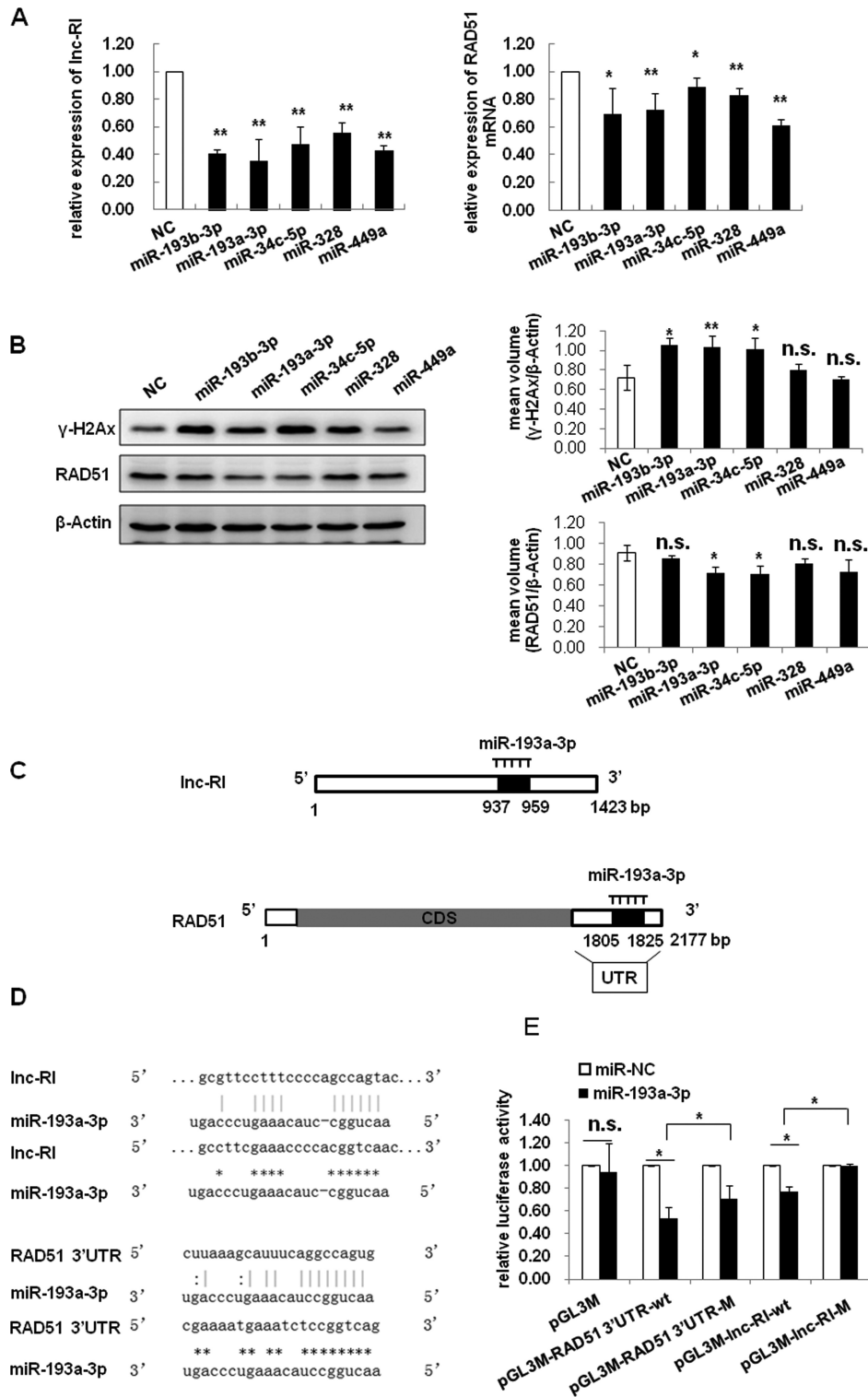
Figure 5. *Lnc-RI* stabilized *RAD51* mRNA by competitively binding to miR-193a-3p. (A, B) Inhibition of *RAD51* and *lnc-RI* expression induced by enforced expression of miR-193b-3p, miR-193a-3p, miR-34c-5p, miR-328-3p or miR-449a. HeLa cells were transfected with synthetic miRNA mimics (100 nM). After 48 h, expression of *lnc-RI* (**A**, left) and *RAD51* (**A right**) was measured by real-time PCR. (**B**) RAD51 and γ-H2Ax protein expression were detected by Western blot and quantified using Quantity One software normalized to β-Actin. (C–E) MiR-193a-3p directly targets the *RAD51* mRNA 3′UTR and *lnc-RI*. (**C**) Predicted target sites of miR-193a-3p in *lnc-RI* and the *RAD51* mRNA 3′UTR. (**D**) Luciferase reporter vectors were constructed by cloning the wild-type *lnc-RI* and *RAD51* mRNA 3′UTR sequences, or mutated *lnc-RI* (937–959 bp) and *RAD51* 3′ UTR (704–724 bp) sequences into the pGL3M plasmid. (**E**) HeLa cells were co-transfected with the reporter vectors and miR-193a-3p or NC. Luciferase activity was analyzed at 48 h after transfection. *t*-test, data are mean ± SD, *n* = 3, *P < 0.05, **P < 0.01, n.s. means no significance.

***Lnc-RI* regulated stability of *RAD51* mRNA by competitive binding with miR-193a-3-p**

MiRNAs bind to the 3′UTR region of target mRNA molecules to facilitate their degradation. LncRNAs have been reported to bind miRNAs competitively to regulate mRNA stability (24). Knockdown of *lnc-RI* facilitated degradation of *RAD51* mRNA (Figure 4C). Furthermore, knockdown of *RAD51* mRNA also depressed *lnc-RI* expression, indicating that *lnc-RI* may regulate *RAD51* mRNA stability by competitively binding certain miRNAs (Supplementary Figure S6).

By searching the open databases RegRNA2.0, TargetScan, miRDB, miRTarBase, starBase v2.0, and microRNA.org-Targets and Expression, five candidate miRNAs (miR-328, miR-193a-3p, miR-193b-3p, miR-34c-5p, and miR-449a) were predicted to target both *RAD51* mRNA 3′UTR sequences and *lnc-RI*, all of which have been reported to influence tumor carcinogenesis or DDR (Table 2). The predicted targeting sites of these miRNAs in *lnc-RI* or *RAD51* gene sequences are shown in Supplementary Figure S9.

HeLa cells were transfected with mimics of the five candidate miRNAs respectively (Supplementary Table S3) and the expression of *lnc-RI* and *RAD51* was detected by real-time PCR or Western blot analysis. As shown in Figure 5A, all five miRNA mimics depressed expression of both *lnc-RI* and *RAD51* at the RNA level. Furthermore, miR-193a-3p and miR-34c-5p were found to mediate the most significant inhibition of RAD51 protein expression, with concomitantly increased γ-H2AX (Figure 5B). These results implicated miR-193a-3p and miR-34c-5p may be the miRNAs through which *lnc-RI* regulates *RAD51* mRNA stabilization.

To confirm direct interactions of the miRNAs (miR-193a-3p and miR-34c-5p), the sequences of *lnc-RI* or the 3′UTR region of *RAD51* mRNA containing the miR-193a-3p or miR-34c-5p binding sites were cloned separately into downstream of the luciferase gene of the pGL3M plasmid (Figure 5C and D). HeLa cells were then co-transfected with these reporter plasmids and miR-193a-3p or miR-34c-5p. While miR-193a-3p significantly suppressed the luciferase activity of both candidate target sequences (Figure 5E), miR-34c-5p has no effect on either candidate target sequence (data not shown). Thus, we focused on miR-193a-3p in further mechanistic studies.

We mutated the binding sites of miR-193a-3p in the sequences of the *lnc-RI* and the 3′UTR region of *RAD51* mRNA before cloning into pGL3M for similar comparative analyses (Figure 5D). As shown in Figure 5E, analysis of relative luciferase activity at 48 h after co-transfection of HeLa cells with the constructed plasmids and miR-193a-3p mimics (or negative control mimics) revealed that mutation of miR-193a-3p binding site attenuated the suppression of luciferase activity of both candidate target sequences mediated by miR-193a-3p in cells transfected with the *lnc-RI*-wt and *RAD51* 3′UTR-wt constructs. However, the *RAD51* mRNA 3′UTR 704–724 bp mutant did not completely relieve the repressive effects of miR-193a-3p on *RAD51* 3′UTR associated luciferase activity, indicating the possible existence of other miR-193a-3p target sites in the

RAD51 mRNA 3′UTR sequence. These results indicated that miR-193a-3p regulates the expressions of *lnc-RI* and *RAD51* by direct interaction.

DISCUSSION

In the present study, a significant negative correlation between endogenous lncRNA *lnc-RI* expression and spontaneous micronucleus frequency was identified, and knockdown of *lnc-RI* was shown to significantly increase DSB accumulation in multiple cell types. We revealed that *lnc-RI* plays a role in the HR pathway of DSB repair though regulation of *RAD51* mRNA stabilization via competition with miR-193a-3p for binding to the 3′UTR region. *Lnc-RI* functions as a ceRNA to relieve the inhibitory effects of miR-193a-3p on *RAD51* expression. These findings provide strong evidence in support of a key role for *lnc-RI* in the maintenance of genome stability.

HR is generally considered to be a dominant error-free mechanism of DSB repair during the late S and G2 phases. RAD51, which catalyzes DNA strand invasion and leads to the formation of a physical structure known as a 'D-loop' between the invading DNA substrate and its homologous DNA sequences, is a critical component of the HR pathway. Dysfunction in RAD51 expression results in deficiency in HR for DSB repair, leading to chromosome aberration, and even embryonic lethality or carcinogenesis (16,39,40). LncRNAs have recently emerged as epigenetic regulatory molecules that play important roles in diverse biological processes and in disease development. However, reports of the involvement of lncRNAs in the HR pathway are relatively rare. In 2015, the lncRNA *TODRA*, a transcript derived from 69 bp upstream of the *RAD51* transcription start site (TSS), was reported to regulate HR repair in a *RAD51*-dependent manner. To date, *TODRA* is the only *RAD51*-associated lncRNA reported to be involved in HR regulation, although no direct interaction between these two genes was identified (33). In the present study, we demonstrated that *lnc-RI* is a novel lncRNA involved in the regulation of HR repair. Knockdown of *lnc-RI* expression caused a marked decline in HR efficiency and increased the accumulation of spontaneous DSBs. Expression levels of several critical regulators of HR activity, including RAD51, RAD50, BRCA1 and BRCA2, were found to be depressed by *lnc-RI* knockdown. As a key protein of HR, RAD51 expression is highest during S/G2 phase of cell cycle (41). So, the decrease of populations of S-phase cells may cause RAD51 reduction. Then we analyzed the cell cycle distribution of HeLa cells after knockdown of *lnc-RI*. As shown in Supplementary Figure S10, knockdown of *lnc-RI* induced G$_2$/M arrest but had no effect on populations of cells in S phase, which indicated that RAD51 reduction is not due to decrease of populations of S phase cells. In accordance with this, the expression of *lnc-RI* showed a negative correlation with micronucleus frequency, which is considered to be a credible biomarker of genomic instability.

LncRNA regulates the expression of target genes through a variety of interactions including RNA-protein, RNA-DNA or RNA-RNA (42,43). It is now widely accepted that lncRNAs act as ceRNA by functioning as decoys of miRNAs, which are a group of small regulatory ncR-

Table 2. Bioinformatic predicted miRNAs target *lnc-RI* and *RAD51*

Target lnc-RI		Target RAD51 3′UTR	
MiRNAs	Database	MiRNAs	Database
miR-3192	RegRNA2.0	miR-3652	miRDB
miR-328 #		miR-4430	
miR-532-3p		miR-532-3p	
miR-134-5p	TargetScan	miR-193b-3p	miRTarBase
miR-148a-3p		miR-3192-5p	
miR-148b-3p		miR-328-3p #	
miR-152-3p		miR-384	
miR-193a-3p #		miR-5571-3p	
miR-193b-3p #		miR-6819-3p	
miR-3118		miR-6840-3p	
miR-34c-5p #		miR-6877-3p	
miR-3652		miR-7975	
miR-384			
miR-4430		miR-134-5p	starBase v2.0
miR-449a #		miR-148a-3p	
miR-5571-3p		miR-148b-3p	
miR-6819-3p		miR-152-3p	
miR-6840-3p		miR-3118	
miR-6877-3p		miR-34c-5p #	
miR-7975		miR-449a	
miR-384	microRNA.org-Targets and Expression	miR-193a-3p #	microRNA.org-Targets and Expression
miR-449a #			
miR-34c-5p #			

Annotations: pounds signed miRNAs were selected for further investigations.
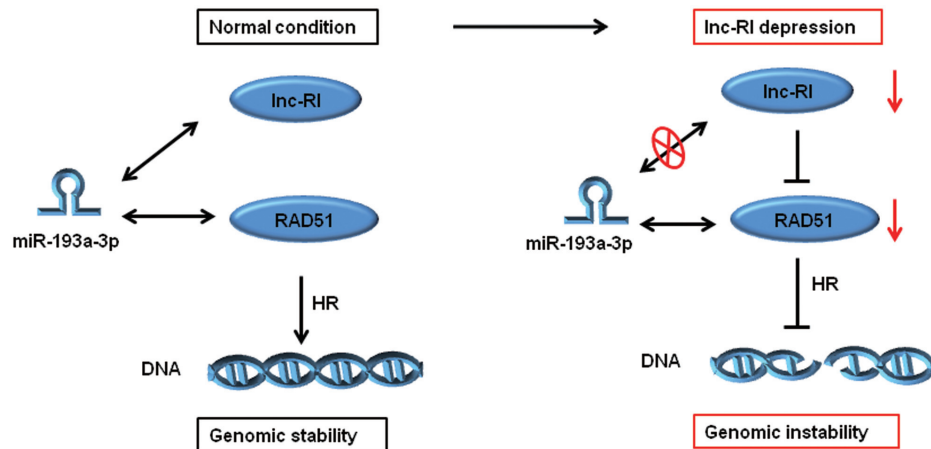
Figure 6. Schematic diagram of the interaction between miR-193a-3p and *lnc-RI* or *RAD51* in the regulation of HR and genomic stability.

NAs comprising ∼22 nucleotides and specifically targeting mRNA 3′UTR or lncRNA sequences to induce gene silencing (24,26,44). In our study, RNAi-mediated *lnc-RI* depression accelerated the degradation of RAD51 mRNA. Furthermore, knockdown of *lnc-RI* or *RAD51* led mutual suppression. Based on the 'ceRNA' hypothesis, we performed bioinformatics analyses that revealed a number of miRNAs with the potential to target both *lnc-RI* and the *RAD51* mRNA 3′UTR. MiR-193a-3p is involved in the pathogenesis of various tumors, and it negatively regulates DDR by targeting the *ING5* gene (45–47). Our results showed that enforced expression of miR-193a-3p mimics inhibited the expression of both *lnc-RI* and *RAD51*, and consequently enhanced DNA damage as indicated by increased γ-H2AX expression. Furthermore, dual luciferase reporter assays confirmed a direct interaction between miR-193a-3p and its predicted target sites in the *lnc-RI* 937–959 bp region and in the *RAD51* mRNA 3′UTR 704–724 bp region. Thus, these findings suggest that *lnc-RI* regulates *RAD51* expression through competitive binding with miR-193a-3p as a ceRNA.

In the present and previous studies, knockdown of *lnc-RI* was also shown to depress the expression of PLK1, which has been reported to promote RAD51 activity via phosphorylation at S14 in response to DNA damage (18,34). In the current study however, we did not explore the ability of *lnc-RI* to regulate RAD51 recombinase activity in a PLK1-dependent manner.

Our studies show that under normal conditions, an appropriate level of *lnc-RI* is necessary to maintain effective

HR repair activity via regulation of *RAD51* expression. *Lnc-RI* regulates *RAD51* mRNA stability by competitively and specifically binding to miR-193a-3p as a ceRNA and relieves its inhibitory effects on the *RAD51* mRNA target. Based on our findings, we propose a model in which depression of *lnc-RI* expression leads to an enhanced interaction between miR-193a-3p and the *RAD51* mRNA 3′UTR, which accelerates the degradation of *RAD51* mRNA to suppress *RAD51* expression, eventually inducing DNA damage through HR repair deficiency (Figure 6).

In summary, our study demonstrates a novel role for the lncRNA *lnc-RI* in the HR pathway of DSB repair. Knockdown of *lnc-RI* suppressed HR repair efficiency and induced the accumulation of spontaneous DSBs. These data indicate that *lnc-RI* functions as a ceRNA to regulates the expression of *RAD51* via the *lnc-RI*/miR-193a-3p/*RAD51* axis. This evidence implicates *lnc-RI* as a novel regulator of the HR pathway that plays an important role in the maintenance of genome stability.

AVAILABILITY

RegRNA2.0 (http://regrna2.mbc.nctu.edu.tw/), TargetScan (http://www.targetscan.org/vert_71/), miRDB (http://www.mirdb.org/), miRTarBase (http://mirtarbase.mbc.nctu.edu.tw/), starBase v2.0 (http://starbase.sysu.edu.cn/), and microRNA.org-Targets and Expression (http://www.microrna.org/microrna/home.do) are open sources for microRNA searching.

SUPPLEMENTARY DATA

Supplementary Data are available at NAR online.

REFERENCES

1. Moore,J.L., Rush,L.M., Breneman,C., Mohideen,M.A. and Cheng,K.C. (2006) Zebrafish genomic instability mutants and cancer susceptibility. *Genetics*, **174**, 585–600.
2. Tubbs,A. and Nussenzweig,A. (2017) Endogenous DNA damage as a source of genomic instability in cancer. *Cell*, **168**, 644–656.
3. Stratton,M.R., Campbell,P.J. and Futreal,P.A. (2009) The cancer genome. *Nature*, **458**, 719–724.
4. Jackson,S.P. and Bartek,J. (2009) The DNA-damage response in human biology and disease. *Nature*, **461**, 1071–1078.
5. Katyal,S., Lee,Y., Nitiss,K.C., Downing,S.M., Li,Y., Shimada,M., Zhao,J., Russell,H.R., Petrini,J.H., Nitiss,J.L. *et al.* (2014) Aberrant topoisomerase-1 DNA lesions are pathogenic in neurodegenerative genome instability syndromes. *Nat. Neurosci.*, **17**, 813–821.
6. Tomé,S., Manley,K., Simard,J.P., Clark,G.W., Slean,M.M., Swami,M., Shelbourne,P.F., Tillier,E.R., Monckton,D.G., Messer,A. *et al.* (2013) MSH3 polymorphisms and protein levels affect CAG repeat instability in Huntington's disease mice. *PLoS Genet.*, **9**, e1003280.
7. López-Otín,C., Blasco,M.A., Partridge,L., Serrano,M. and Kroemer,G. (2013) The hallmarks of aging. *Cell*, **153**, 1194–1217.
8. Aguilera,A. and García-Muse,T. (2013) Causes of genome instability. *Annu. Rev. Genet.*, **47**, 1–32.
9. Jeggo,P.A., Pearl,L.H. and Carr,A.M. (2016) DNA repair, genome stability and cancer: a historical perspective. *Nat. Rev. Cancer*, **16**, 35–42.
10. Aguilera,A. and Gómez-González,B. (2008) Genome instability: a mechanistic view of its causes and consequences. *Nat. Rev. Genet.*, **9**, 204–217.
11. Wickramasinghe,V.O. and Venkitaraman,A.R. (2016) RNA processing and genome stability: cause and consequence. *Mol. Cell*, **61**, 496–505.
12. Saintigny,Y., Delacôte,F., Varès,G., Petitot,F., Lambert,S., Averbeck,D. and Lopez,B.S. (2001) Characterization of homologous recombination induced by replication inhibition in mammalian cells. *EMBO J.*, **20**, 3861–3870.
13. Li,W., Li,F., Huang,Q., Shen,J., Wolf,F., He,Y., Liu,X., Hu,Y.A., Bedford,J.S. and Li,C.Y. (2011) Quantitative, noninvasive imaging of radiation-induced DNA double-strand breaks in vivo. *Cancer Res.*, **271**, 4130–4137.
14. Sung,P. (1994) Catalysis of ATP-dependent homologous DNA pairing and strand exchange by yeast RAD51 protein. *Science*, **265**, 1241–1243.
15. Baumann,P., Benson,F.E. and West,S.C. (1996) Human Rad51 protein promotes ATP-dependent homologous pairing and strand transfer reactions in vitro. *Cell*, **87**, 757–766.
16. Cousineau,I., Abaji,C. and Belmaaza,A. (2005) BRCA1 regulates RAD51 function in response to DNA damage and suppresses spontaneous sister chromatid replication slippage: implications for sister chromatid cohesion, genome stability, and carcinogenesis. *Cancer Res.*, **65**, 11384–11391.
17. Abaji,C., Cousineau,I. and Belmaaza,A. (2005) BRCA2 regulates homologous recombination in response to DNA damage: implications for genome stability and carcinogenesis. *Cancer Res.*, **65**, 4117–4125.
18. Yata,K., Lloyd,J., Maslen,S., Bleuyard,J.Y., Skehel,M., Smerdon,S.J. and Esashi,F. (2012) Plk1 and CK2 act in concert to regulate Rad51 during DNA double strand break repair. *Mol. Cell*, **45**, 371–383.
19. Krejci,L., Altmannova,V., Spirek,M. and Zhao,X. (2012) Homologous recombination and its regulation. *Nucleic Acids Res.*, **40**, 5795–5818.
20. Kawasaki,Y., Komiya,M., Matsumura,K., Negishi,L., Suda,S., Okuno,M., Yokota,N., Osada,T., Nagashima,T., Hiyoshi,M. *et al.* (2016) MYU, a target lncRNA for Wnt/c-Myc signaling, mediates induction of CDK6 to promote cell cycle progression. *Cell Rep.*, **16**, 2554–2564.
21. Wang,K., Long,B., Zhou,L.Y., Liu,F., Zhou,Q.Y., Liu,C.Y., Fan,Y.Y. and Li,P.F. (2014) CARL lncRNA inhibits anoxia-induced mitochondrial fission and apoptosis in cardiomyocytes by impairing miR-539-dependent PHB2 downregulation. *Nat. Commun.*, **5**, 3596.
22. Grote,P., Wittler,L., Hendrix,D., Koch,F., Währisch,S., Beisaw,A., Macura,K., Bläss,G., Kellis,M., Werber,M. *et al.* (2013) The tissue-specific lncRNA Fendrr is an essential regulator of heart and body wall development in the mouse. *Dev. Cell*, **24**, 206–214.
23. Savić,N., Bär,D., Leone,S., Frommel,S.C., Weber,F.A., Vollenweider,E., Ferrari,E., Ziegler,U., Kaech,A., Shakhova,O. *et al.* (2014) LncRNA maturation to initiate heterochromatin formation in the nucleolus is required for exit from pluripotency in ESCs. *Cell Stem Cell*, **15**, 720–734.
24. Cesana,M., Cacchiarelli,D., Legnini,I., Santini,T., Sthandier,O., Chinappi,M., Tramontano,A. and Bozzoni,I. (2011) A long noncoding RNA controls muscle differentiation by functioning as a competing endogenous RNA. *Cell*, **147**, 358–369.

25. Sun,T.T., He,J., Liang,Q, Ren,L.L., Yan,T.T., Yu,T.C., Tang,J.Y., Bao,Y.J., Hu,Y., Lin,Y. *et al.* (2016) LncRNA GClnc1 promotes gastric carcinogenesis and may act as a modular scaffold of WDR5 and KAT2A complexes to specify the histone modification pattern. *Cancer Discov.*, **6**, 784–801.

26. Salmena,L., Poliseno,L., Tay,Y., Kats,L. and Pandolfi,P.P. (2011) A ceRNA hypothesis: the Rosetta Stone of a hidden RNA language? *Cell*, **146**, 353–358.

27. Wang,G., Li,Z., Zhao,Q., Zhu,Y., Zhao,C., Li,X., Ma,Z., Li,X. and Zhang,Y. (2014) LincRNA-p21 enhances the sensitivity of radiotherapy for human colorectal cancer by targeting the Wnt/beta-catenin signaling pathway. *Oncol. Rep.*, **31**, 1839–1845.

28. Jiao,Y., Liu,C., Cui,F.M., Xu,J.Y., Tong,J., Qi,X.F., Wang,L.L. and Zhu,W. (2015) Long intergenic non-coding RNA induced by X-ray irradiation regulates DNA damage response signaling in the human bronchial epithelial BEAS-2B cell line. *Oncol. Lett.*, **9**, 169–176.

29. Liu,X., Li,D., Zhang,W., Guo,M. and Zhan,Q. (2012) Long non-coding RNA gadd7 interacts with TDP-43 and regulates Cdk6 mRNA decay. *EMBO J.*, **31**, 4415–4427.

30. Zhang,Y., He,Q., Hu,Z., Feng,Y., Fan,L., Tang,Z., Yuan,J., Shan,W., Li,C., Hu,X. *et al.* (2016) Long noncoding RNA LINP1 regulates repair of DNA double-strand breaks in triple-negative breast cancer. *Nat. Struct. Mol. Biol.*, **23**, 522–530.

31. Prensner,J.R., Chen,W., Iyer,M.K., Cao,Q., Ma,T., Han,S., Sahu,A., Malik,R., Wilder-Romans,K., Navone,N. *et al.* (2014) PCAT-1, a long noncoding RNA, regulates BRCA2 and controls homologous recombination in cancer. *Cancer Res.*, **74**, 1651–1660.

32. Sharma,V., Khurana,S., Kubben,N., Abdelmohsen,K., Oberdoerffer,P., Gorospe,M. and Misteli,T. (2015) A BRCA1-interacting lncRNA regulates homologous recombination. *EMBO Rep.*, **16**, 1520–1534.

33. Gazy,I., Zeevi,D.A., Renbaum,P., Zeligson,S., Eini,L., Bashari,D., Smith,Y., Lahad,A., Goldberg,M., Ginsberg,D. *et al.* (2015) TODRA, a lncRNA at the RAD51 locus, is oppositely regulated to RAD51, and enhances RAD51-dependent DSB (double strand break) repair. *PLoS One*, **10**, e0134120.

34. Wang,Z.D., Shen,L.P., Chang,C., Zhang,X.Q., Chen,Z.M., Li,L., Chen,H. and Zhou,P.K. (2016) Long noncoding RNA lnc-RI is a new regulator of mitosis via targeting miRNA-210-3p to release PLK1 mRNA activity. *Sci. Rep.*, **6**, 25385.

35. Wang,Z.D., Zhang,X.Q., Du,J., Lu,X., Wang,Y., Tian,R., Liu,Q.J. and Chen,Y. (2015) Continuous cytogenetic follow-up, over 5 years, of three individuals accidentally irradiated by a cobalt-60 source. *Mutat. Res. Genet. Toxicol. Environ. Mutagen.*, **779**, 1–4.

36. Chan,N., Koritzinsky,M., Zhao,H., Bindra,R., Glazer,P.M., Powell,S., Belmaaza,A., Wouters,B. and Bristow,R.G. (2008) Chronic hypoxia decreases synthesis of homologous recombination proteins to offset chemoresistance and radioresistance. *Cancer Res.*, **68**, 605–614.

37. Seluanov,A, Mittelman,D, Pereira-Smith,OM, Wilson,JH and Gorbunova,V. (2004) DNA end joining becomes less efficient and more error-prone during cellular senescence. *Proc. Natl. Acad. Sci. U.S.A.*, **101**, 7624–7629.

38. Fenech,M. and Morley,A.A. (1985) Measurement of micronuclei in lymphocytes. *Mutat. Res.*, **147**, 29–36.

39. Shinohara,A., Ogawa,H. and Ogawa,T. (1992) Rad51 protein involved in repair and recombination in S. cerevisiae is a RecA-like protein. *Cell*, **69**, 457–470.

40. Lim,D.S. and Hasty,P. (1996) A mutation in mouse rad51 results in an early embryonic lethal that is suppressed by a mutation in p53. *Mol. Cell Biol.*, **16**, 7133–7143.

41. Somyajit,K., Saxena,S., Babu,S., Mishra,A. and Nagaraju,G. (2015) Mammalian RAD51 paralogs protect nascent DNA at stalled forks and mediate replication restart. *Nucleic Acids Res.*, **43**, 9835–9855.

42. Rinn,J.L. and Chang,H.Y. (2012) Genome regulation by long noncoding RNAs. *Annu. Rev. Biochem.*, **81**, 145–166.

43. Mercer,T.R., Dinger,M.E. and Mattick,J.S. (2009) Long non-coding RNAs: insights into functions. *Nat. Rev. Genet.*, **10**, 155–159.

44. Lee,R.C., Feinbaum,R.L. and Ambros,V. (1993) The C. elegans heterochronic gene lin-4 encodes small RNAs with antisense complementarity to lin-14. *Cell*, **75**, 843–854.

45. Gao,X.N., Lin,J., Li,Y.H., Gao,L., Wang,X.R., Wang,W., Kang,H.Y., Yan,G.T., Wang,L.L. and Yu,L. (2011) MicroRNA-193a represses c-kit expression and functions as a methylation-silenced tumor suppressor in acute myeloid leukemia. *Oncogene*, **30**, 3416–3428.

46. Li,Y., Deng,H., Lv,L., Zhang,C., Qian,L., Xiao,J., Zhao,W., Liu,Q., Zhang,D., Wang,Y. *et al.* (2015) The miR-193a-3p-regulated ING5 gene activates the DNA damage response pathway and inhibits multi-chemoresistance in bladder cancer. *Oncotarget*, **6**, 10195–10206.

47. Williams,M., Kirschner,M.B., Cheng,Y.Y., Hanh,J., Weiss,J., Mugridge,N., Wright,C.M., Linton,A., Kao,S.C., Edelman,J.J. *et al.* (2015) MiR-193a-3p is a potential tumor suppressor in malignant pleural mesothelioma. *Oncotarget*, **6**, 23480–23495.